Electronic Supplementary Material (ESI) for Journal of Materials Chemistry A.

Supplementary information

Understanding Defects and Band Tailing Characteristics and Their Impact on the Device Performance of $Cu_2ZnSn(S,Se)_4$ Solar Cells

Vijay C. Karade[1,†], Mahesh P. Suryawanshi[2,†], Jun Sung Jang[1], Kuldeep Singh Gour[1], Suyoung Jang[1], Jongsung Park[3], Jin Hyeok Kim[1,*], and Seung Wook Shin[4,*]

[1]Optoelectronics Convergence Research Center and Department of Materials Science and Engineering, Chonnam National University, 300, Yongbong-Dong, Buk-Gu, Gwangju 61186, South Korea.

[2]School of Photovoltaic and Renewable Energy Engineering, University of New South Wales, Sydney, NSW, 2052 Australia.

[3]Department of Energy Engineering, Gyeongsang National University, Jinju, 52849, Republic of Korea.

[4]Future Agricultural Research Division, Water Resource and Environment Research Group, Rural Research Institute, Korea Rural Community Corporation, Ansan-Si, Gyeonggi-do 15634, South Korea.

Corresponding Authors

***E-mail:** swshin1211@gmail.com **(S.W. Shin)** and jinhyeok@chonnam.ac.kr **(J.H. Kim)**

† V.C.K. and M.P.S. contributed equally to this work

1. Experimental details

1.1 Deposition of the metallic precursors

Initially, the 2.5 x 2.5 cm^2 sized 1 μm thick Molybdenum (Mo) coated soda-lime glass (SLG) substrates by a direct current (DC) sputtering technique were cleaned ultrasonically by isopropyl alcohol and deionized water for 10 min. and used for further process. For metallic precursor fabrication, the three-inch Copper (Cu), Zinc (Zn), and Tin (Sn) metal targets of 99.999 % purity (TASCO, USA) were used. The DC sputtering conditions of each metallic stacked-layer were as follows; Cu: 0.68 W/cm^2, Sn: 0.68 W/cm^2 and Zn: 1.55~ 0.68 W/cm^2, respectively. The substrates were rotated at 5 rpm/min. during all the sputtering processes with a process base pressure of 8 mTorr and argon (Ar) gas flow of 30 sccm, respectively. The metallic precursors from the A series were prepared sequentially using Cu-Zn layer with deposition times of 1500 s and Cu-Sn layer with deposition times of 900 s, while in the B series, it was prepared sequentially using Cu/Sn/Zn on Mo substrates by a DC magnetron sputtering technique. The substrate holder was cooled using a homemade cooling chuck system, and the substrate temperature was maintained at 5 ℃ to form the smooth morphology of all metallic precursors.[1-4] The sputtering conditions of each metallic layer for A and B series samples are given in Table S1 and S2, respectively.

Table S1. Sample names and metallic precursor deposition conditions for samples A1 to A4. Other sputtering conditions were kept same.

Sample	Sputtering power			Deposition time (s)	
	Zn	Sn	Cu	Cu-Zn	Cu-Sn
A1	50 W	30 W	45 W	900	1500
A2	60 W				
A3	65 W				
A4	70 W				

Table S2. Sample names and metallic precursor deposition for samples B1 to B4. Sputtering powers for Zn, Sn, and Cu targets were 30 W. Other sputtering conditions were kept same.

Sample	Deposition time (s)		
	Zn	Sn	Cu
B1	1800	2000	2800
B2			3000
B3			3200
B4			3400

1.2 Soft-annealing and sulfo-selenization processes of metallic precursors

The pre-annealing (termed “soft-annealing”) treatment under Ar atmosphere was employed for both series of samples to achieve smooth morphologies. The as-deposited metallic stacked precursor was placed at the center of the tube, and before the soft-annealing process, the tube was purged with Ar gas. The ramping rate of the soft-annealing process was fixed to 10 °C /min.,

and then the metallic stacked precursors were heated at a temperature of 300 ℃ for 1 h and allowed to cool down naturally to room temperature after the heating process.[1,2,4]

The soft-annealed metallic stacked precursor thin films were annealed under a mixed S and Se atmosphere to prepare a high-quality CZTSSe absorber layer. The S and Se powders were purchased from Sigma Aldrich (99.999%) and mixed in the S/Se ratio of 1:100. Further, the soft-annealed metallic precursors and 0.2 gm of mixed S and Se powders were placed in a graphite box with a volume of ~ 406 cm^3. The graphite box is subsequently then placed into a chamber-type rapid thermal annealing system, which allows accurate control of the chalcogenide vapor pressure during the annealing process. The chamber was evacuated for base pressure of 8×10^{-5} Torr, and then the chamber pressure was maintained up to 500 Torr with a controlled supply of Ar in the chamber before the annealing process. The complete annealing process was performed for 10 min. at 520 ℃ with the heating rate was 10 ℃/s. After the annealing process, the annealed thin films were naturally cooled for one hour and removed.

1.3 Device fabrication process

The CZTSSe solar cell devices were fabricated with a multi-layered structure of Al/AZO/i-ZnO/CdS/CZTSSe/Mo/SLG. Before deposition of the CdS buffer layer, each CZTSSe thin-film was etched with 0.2 M potassium cyanide at room temperature for 120 s and rinsed using DI water for 60 s. The 50 nm thick CdS buffer layer was deposited onto the absorber layers via the chemical bath deposition method using a precursor solution consisting of 0.0015 M $CdSO_4$, 2.871 M ammonia, and 0.05 M thiourea at 60 °C for 14.5 min. After deposition of the thin CdS buffer layer, the samples were dried for 1 h. The 80 nm *i*-ZnO thin film with high resistivity was prepared using the RF magnetron sputtering technique at room temperature, with an RF power of 50 W, and at a working pressure of 1 mTorr under Ar and O_2 mixed plasma. The 580 nm thick

Al-doped ZnO layers were deposited using the RF sputtering technique at 350 °C, with an RF power of 70 W, and at a working pressure of 1 mTorr under Ar plasma. Finally, the Al top grid was deposited using the DC sputtering technique around 1 μm by keeping the active area of the fabricated solar cells up to 0.3 cm^2. Initially, the contacts were masked properly, then the crystalline MgF_2 powder (99.9% purity) purchased from i-TASCO was used to deposit the MgF_2 anti-reflection layers by the thermal evaporation technique. Then, the MgF_2 granules were placed 1-2 mm thick tungsten boat and the chamber was evacuated to 1×10^{-6} Torr. Finally, the 100 nm thick MgF_2 layer was deposited at an applied current of 40 A by maintaining the deposition rate of 0.1 Å/s.

2. Characterizations of thin films and solar cell devices

The phase purity and structural properties of absorber thin films were measured by high-resolution XRD (X'pert PRO, Philips, Eindhoven, Netherlands) ranging from 5° to 90° and Raman scattering spectroscopy with a micro-Raman spectrometer (HORIBA, JOBIN–YVON HR 800) with a spectral resolution around 0.35 cm^{-1} and a confocal resolution of 100 μm under the backscattering geometry at room temperature. The 514 nm line of an Ar^+ ion laser source was used for excitation, and the incident laser power on the sample surface was around 10 mW. The composite ratio of the CZTSSe thin films was characterized by an X-ray fluorescence (XRF) spectroscopy (Axios Minerals PANalytical Netherlands) calibrated with an internal standard equipment calculation process software. The surface morphology of thin films was characterized using field emission scanning electron microscopy (FE-SEM, Gemini 500 attached in energy-dispersive X-ray spectroscopy (EDS, OXford, AZtecLive). The room temperature photoluminescence (RTPL) and Time-resolved (TRPL) of the thin films were characterized by avalanche photodiode equipment (SH-4 and USA). PL characterizations were performed on the

devices using the time-correlated single-photon counting technique with an excitation wavelength of 514 nm laser. For TRPL spectra, the signal was detected by id110 VIS 100 MHz Photon Detector operated in free-running mode. The two-exponential function was used to fit the normalized PL decay curves and to obtain carrier lifetime. The power conversion efficiency (PCE) and external quantum efficiency (EQE) spectra for solar cell devices were characterized by a class AAA solar simulator (WXS-155S-L2, WACOM, and Japan) with the condition of AM 1.5G, 100 mW/cm^2, and 25 ^{o}C and with an incident photon conversion efficiency (IPCE) measurement unit (PV measurement, Inc., USA), respectively. The room temperature capacitance (C) *vs.* voltage (V) plot of the solar cell devices was collected from -1.5 V to 1 V DC bias voltage by using 25 mV and 100 kHz alternating current (AC) signal. An impedance analyzer (Hewlett Packard, HP4284) is used to perform the C-V measurements.

The junction depletion width (W) is extracted from the C–V plot shown in Fig. S6(b) and (d), following equation (Eq. (1)).

$$C = \frac{\varepsilon_0 \varepsilon_r A}{w} \qquad \text{Eq. (1)}$$

Where ε_0 is free space permittivity, and ε_r is the relative dielectric constant of CZTSSe. The value of C is obtained from Fig. S6 (a) and (c) at V = 0. The ε_r value of 8.2 is obtained from earlier published papers. The area (A) of the solar cell device is used with the number of 3×10^{-5} m^2. Afterward, free carrier concentration (N_a) is calculated following Eq. (2).

$$N = \frac{-2}{q\varepsilon_0 \varepsilon_\gamma A^2 \left[\frac{d\left(C^{-2}\right)}{dv}\right]} - 1 \qquad \text{Eq. (2)}$$

Where q is the electronic charge. The value for $[d(C^{-2})/dV)]^{-1}$ is taken from the slope of $(1/C^2)$–V.

Table S3. Composition data of absorber samples A1 to A4 and B1 to B4 determined from XRF.

Sample	Cu/ (Zn+Sn)	Cu/Sn	Zn/Sn	Cu/Zn	S/ (S+Se)
A1	0.66	1.42	1.15	1.24	0.03
A2	0.57	1.52	1.67	0.91	0.03
A3	0.53	1.41	1.65	0.86	0.04
A4	0.51	1.46	1.87	0.78	0.04
B1	0.58	1.22	1.09	1.11	0.02
B2	0.64	1.35	1.12	1.21	0.05
B3	0.66	1.35	1.05	1.29	0.02
B4	0.71	1.47	1.07	1.37	0.02

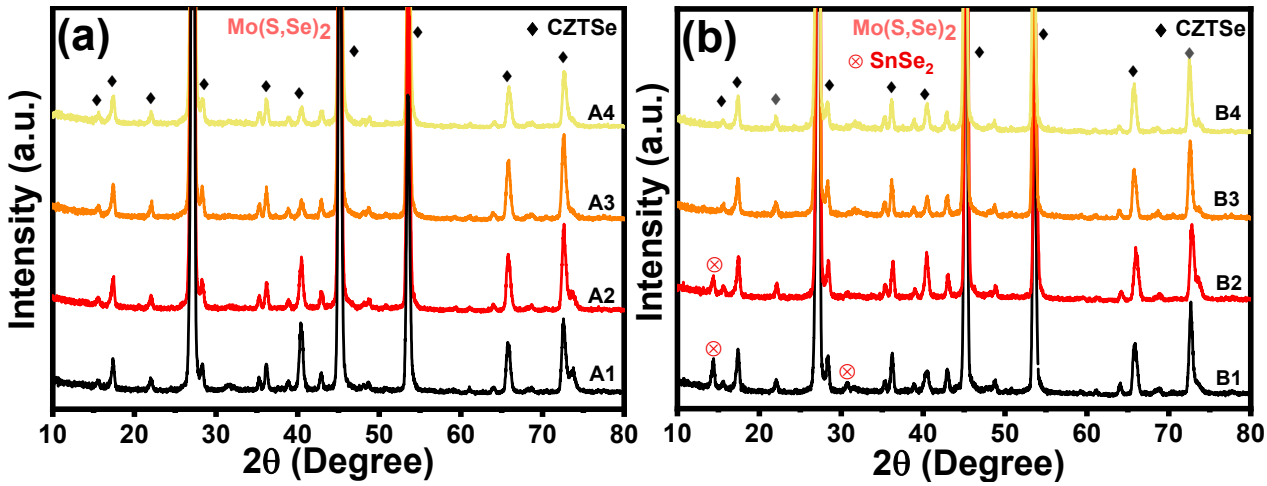

Fig. S1. XRD patterns of the CZTSSe thin films for samples (a) A1 to A4 and (b) B1 to B4 at room temperature. Symbols of `♦`,`●`, and `⊗` are CZTSSe, $Mo(S,Se)_2$, and $SnSe_2$, respectively.

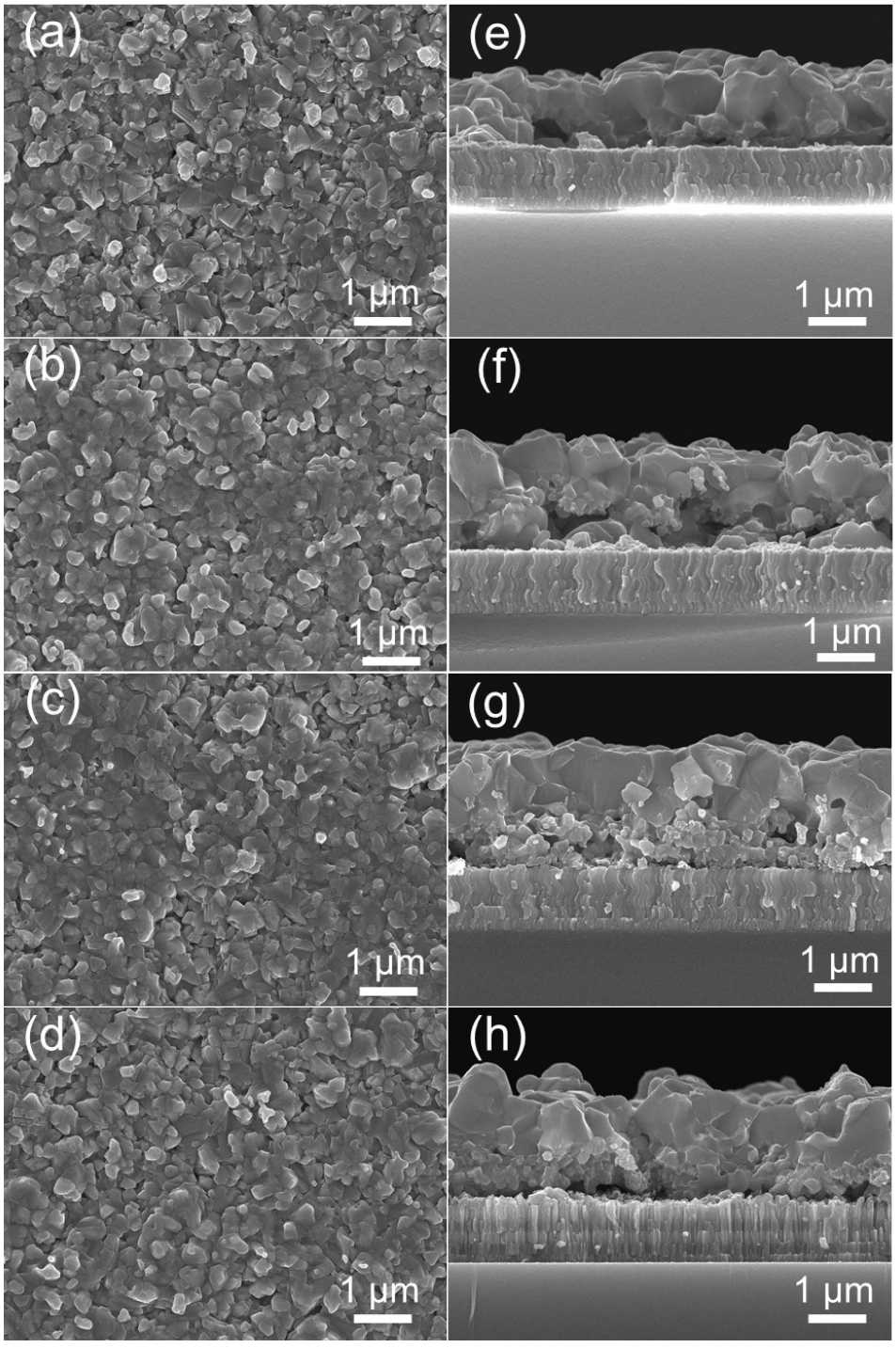

Fig. S2. FE-SEM surface images of the absorber samples (a) A1, (b) A2, (c) A3 and (d) A4, and corresponding cross-sectional images from (e) to (h), respectively.

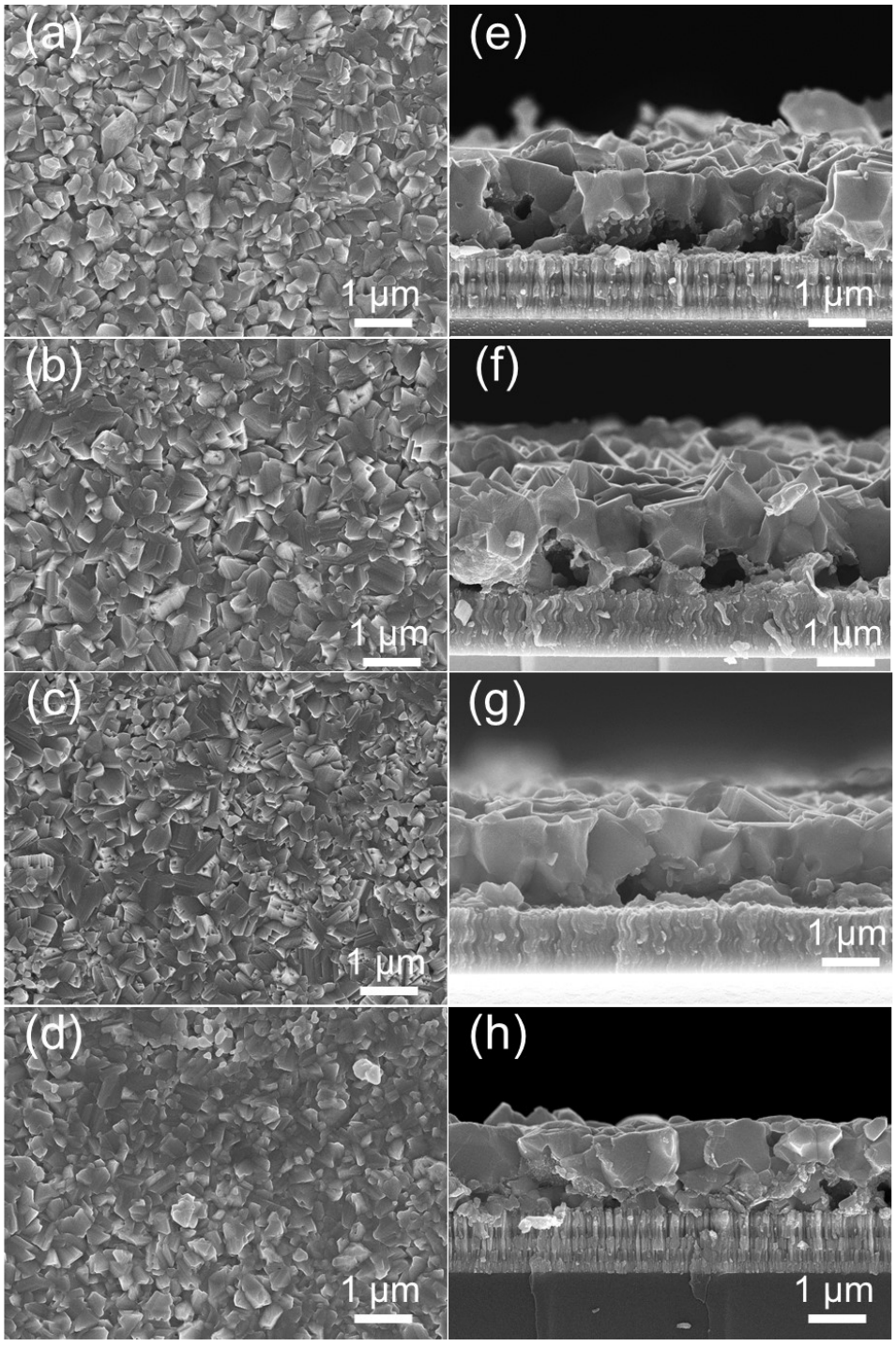

Fig. S3. FE-SEM surface images of the absorber samples (a) B1, (b) B2, (c) B3, and (d) B4 and corresponding cross-sectional images from (e) to (h), respectively.

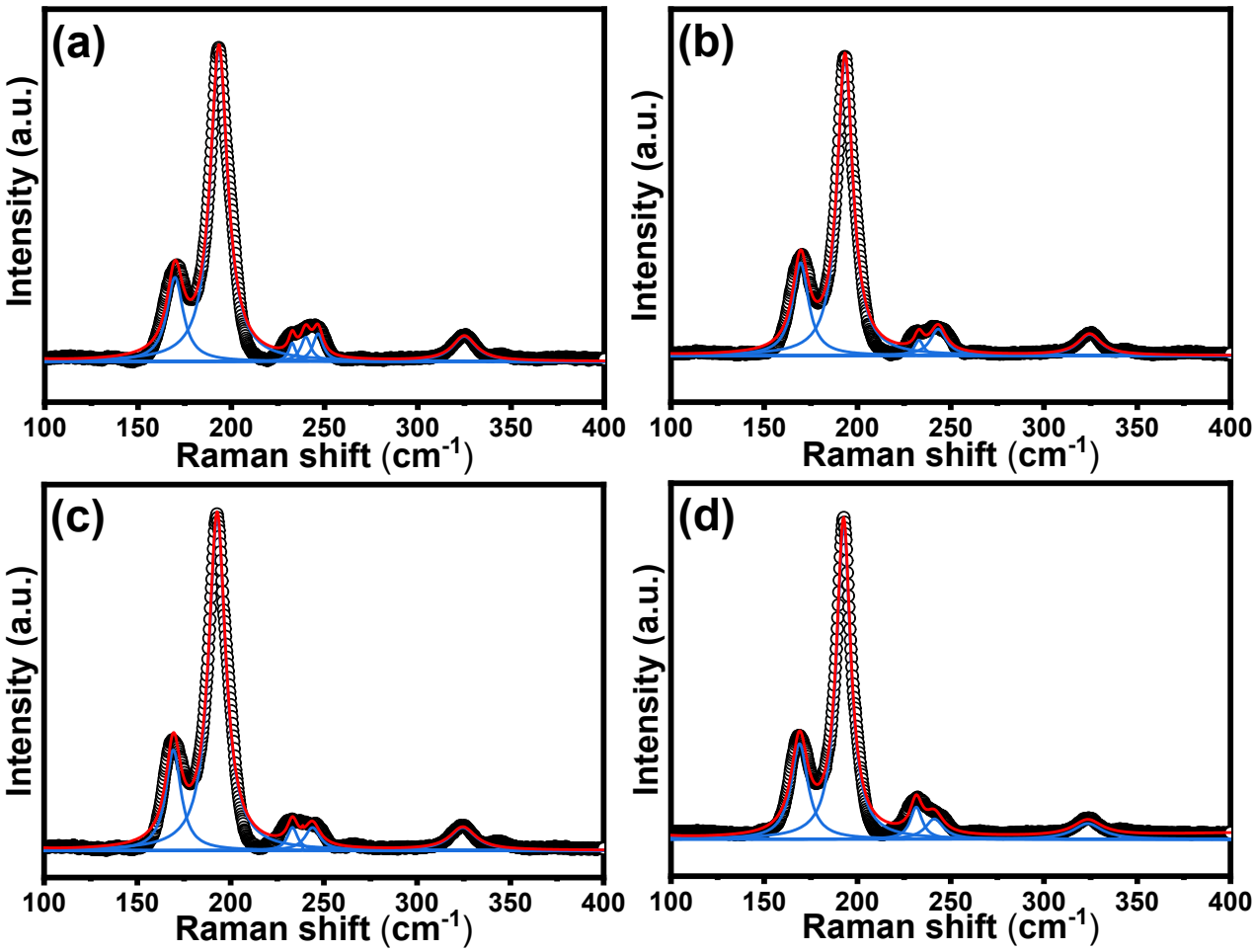

Fig. S4. Raman spectra of samples fitted with the Lorentzian function; (a) A1, (b) A2, (c) A3, and (d) A4.

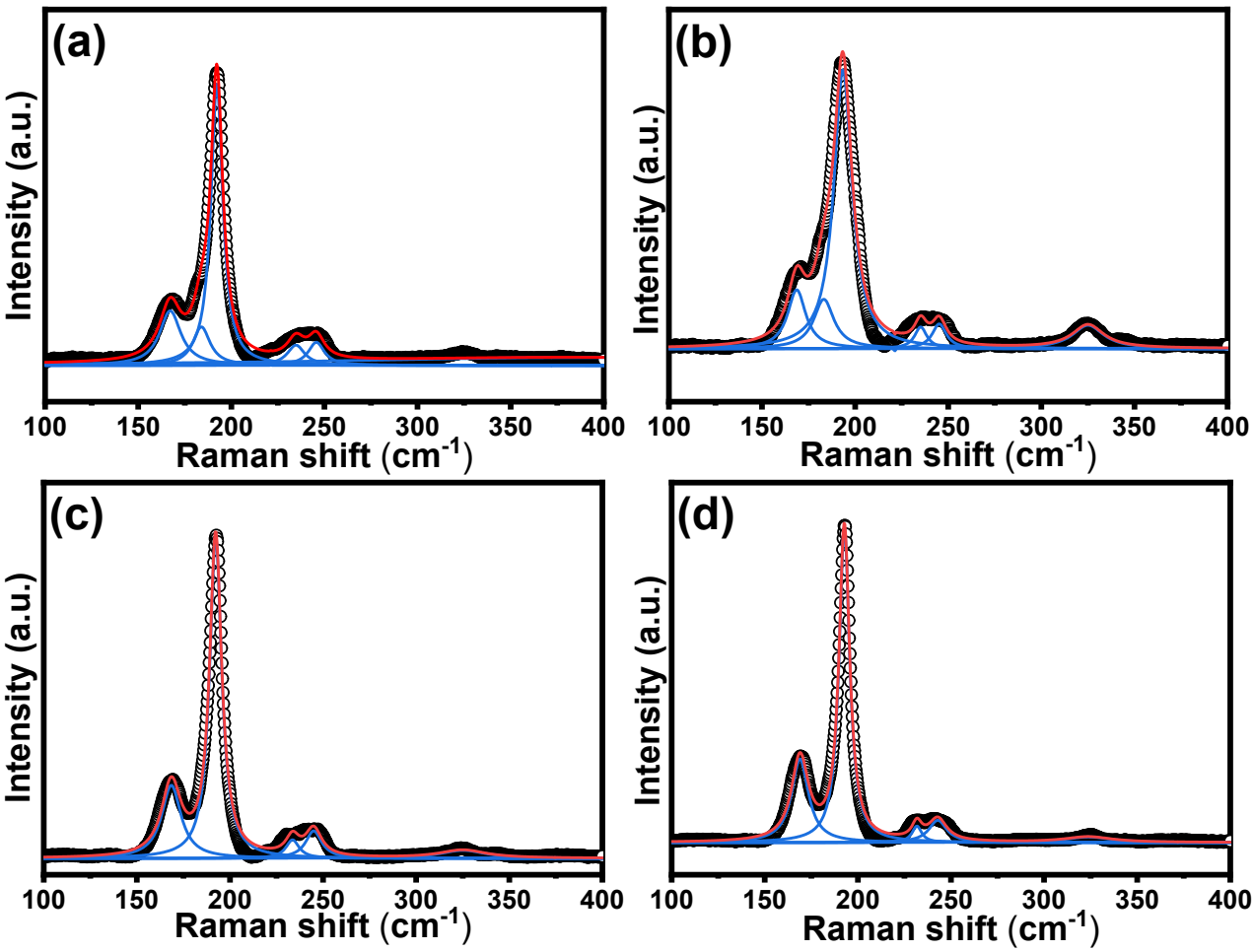

Fig. S5. Raman spectra of samples fitted with the Lorentzian function; (a) B1, (b) B2, (c) B3, and (d) B4.

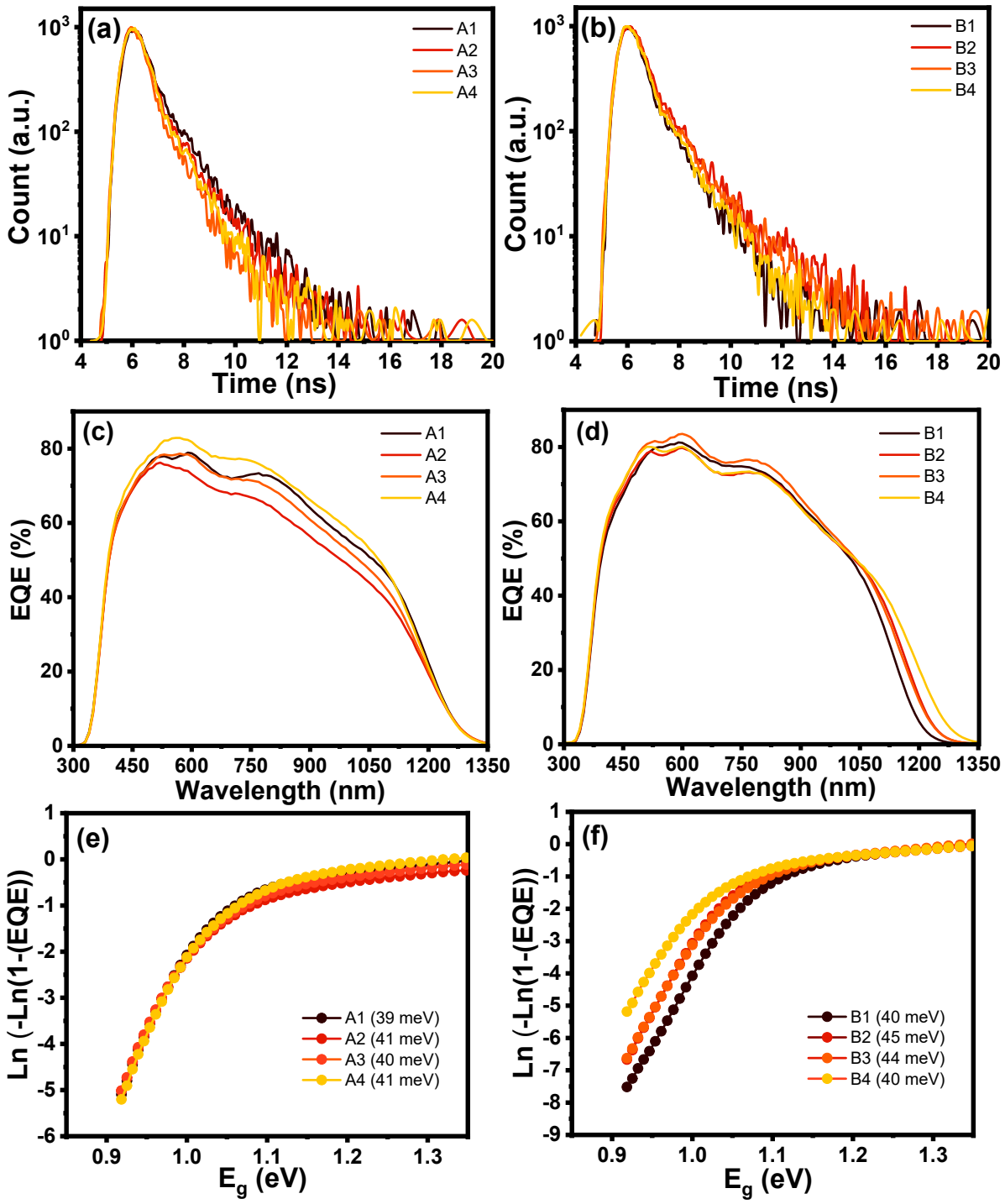

Fig. S6. ((a)-(b)) *TRPL* spectra, ((c)-(d)) EQE response and ((e)-(f)) Urbach energy plot of the best performing CZTSSe solar cells from the A and B series. The EQE spectra measured for the A and B series do not have an ARC coating over the device.

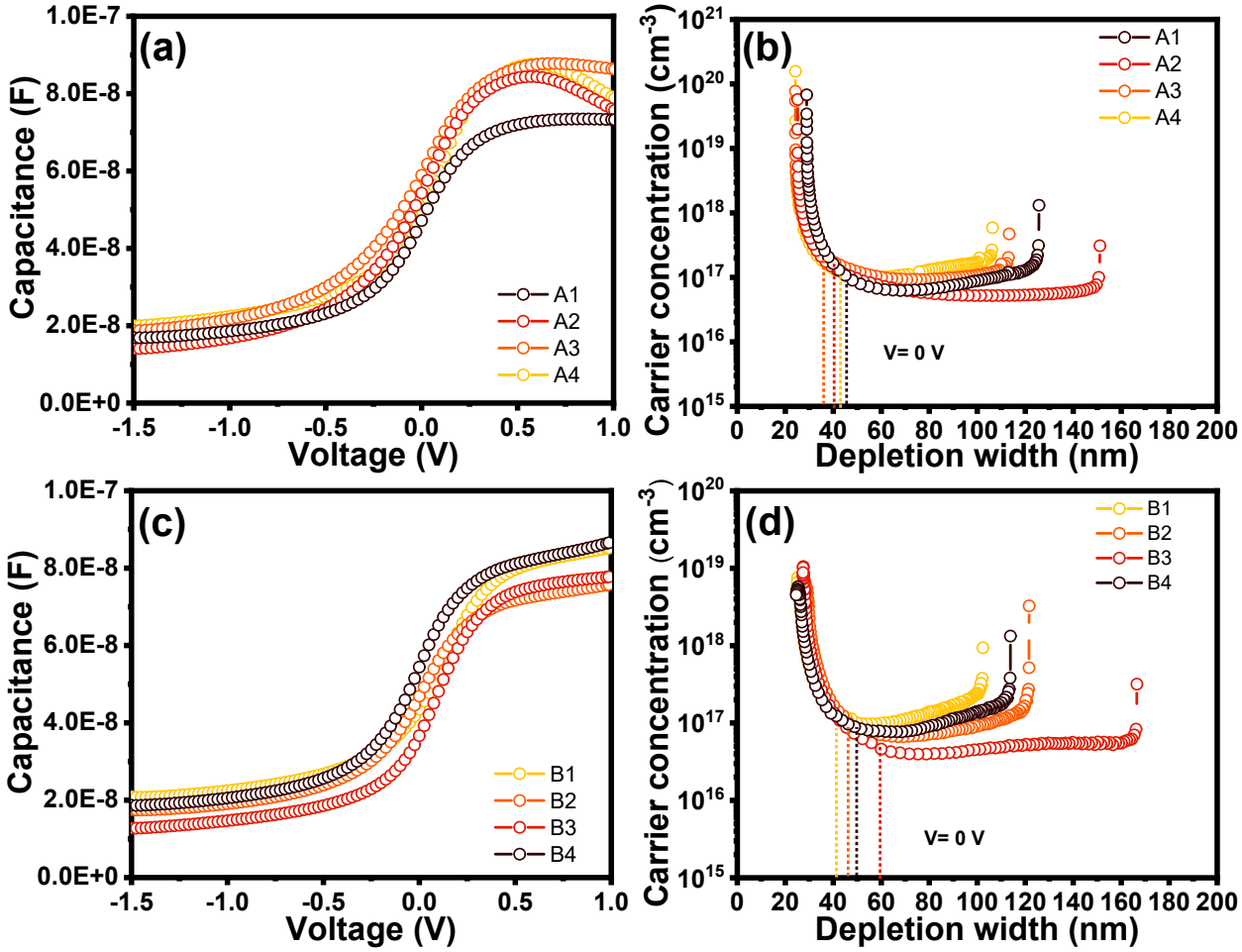

Fig. S7. ((a)-(c)) *C-V* plots and ((b)-(d)) N_a *vs.* depletion width (W_d) of the best performing CZTSSe solar cells from the series A and B samples.

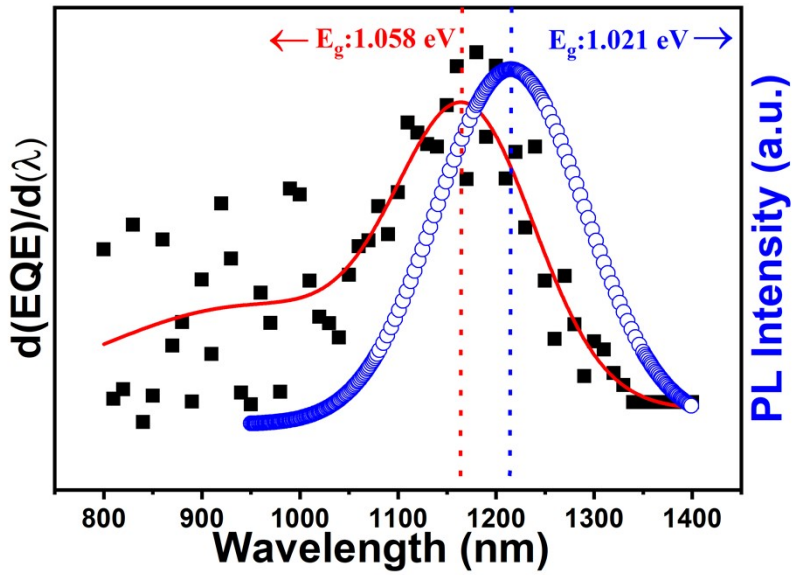

Fig. S8. Band tailing characteristics established from *d*EQE/*dλ vs.* wavelength and RTPL plots in samples, *d*EQE/*dλ* (black square), gauss fitted *d*EQE/*dλ* (red line), and Gaussian fitted RTPL spectra (blue circles) of the champion CZTSSe solar cell.

References

1. M. G. Gang, V. C. Karade, M. P. Suryawanshi, H. Yoo, M. He, X. Hao, I. J. Lee, B. H. Lee, S. W. Shin and J. H. Kim, *ACS Appl. Mater. Interfaces*, 2021, **13**, 3959–3968
2. V. Karade, E. Choi, M. G. Gang, H. Yoo, A. Lokhande, P. Babar, J. S. Jang, J. Seidel, J. S. Yun, J. Park and J. H. Kim, *ACS Appl. Mater. Interfaces*, 2021, **13**, 429–437
3. M. G. Gang, S. W. Shin, C. W. Hong, K. V. Gurav, J. Gwak, J. H. Yun, J. Y. Lee and J. H. Kim, *Green Chem.*, 2016, **18**, 700–711
4. M. G. Gang, S. W. Shin, M. P. Suryawanshi, U. V. Ghorpade, Z. Song, J. S. Jang, J. H. Yun, H. Cheong, Y. Yan and J. H. Kim, *J. Phys. Chem. Lett.*, 2018, **9**, 4555–4561